International Journal of I.C. Engines and Gas Turbines
Vol. 4: Issue 2
www.journalspub.com

Numerical Techniques Applied on Hydrostatic Bearing using Computational Fluid Dynamics

Harshvardhan Ojha[1], Naman Gargayan*[1], Swamy Bhavesh[2], Viral Mali[2], Snehal Patel[3]*
[1]Department of Mechanical Engineering, Navrachana University, Vadodara, Gujarat, India
[2]Department of Mechanical Engineering, Navrachana University, Vadodara, Gujarat, India
[3]M.Tech (Thermal Science and Engineering), Department of Mechanical Engineering, Indian Institute of Technology Kharagpur, Kharagpur, West Bengal, India

ABSTRACT

In hydrostatic bearing, the oil or lubricant is supplied to the required place in bearing from external source that place is the recess. The oil enters axially and leaves perpendicularly. The important task for the purpose of analysis is finding pressure distribution in the recess. The problem here is that, it is possible to find out analytical solution for one dimension, but it is not possible to find out pressure distribution in the recess for two-dimensions.

Keywords: Oil, computational fluid dynamics, lubricant, hydrostatic bearing

Corresponding Author
E-mail: vardhanharsh412@gmail.com; namangargayan@gmail.com

INTRODUCTION

Hydrostatic or hydrodynamic are fluid film bearing that depend on the lubrication such as oil or water to avoid metal to metal contact between the moving and stationary elements. Since the friction is almost negligible so the generation of heat is due to the oil shear. Here the weight of the shaft is supported by the pressurized liquid that is present between the contact surfaces. The pressurized lubrication is supplied by the pump from the bottom of the bearing. In such bearing, lubrication used is generally air water or oil. The main advantage of this bearing that at any speed even at zero rpm metal to metal contact is avoided so the torque required to attained the desired speed is low.

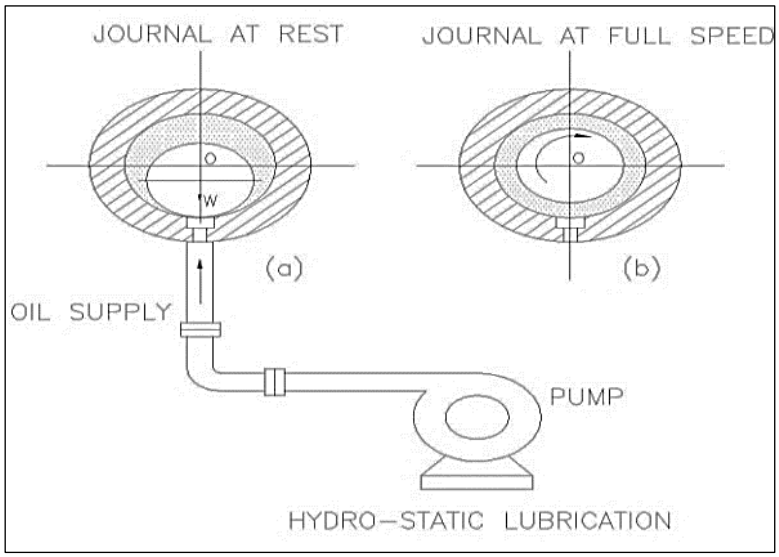

Fig. 1: *(a) Journal at rest, (b) Journal at full speed.*

Such bearing are also termed as 'externally pressurized bearing'. As shown in the above Figure 1 when the journal is at rest there is no supply of oil but as soon as the shaft starts to rotate the oil is supplied externally at high pressure into the clearance zone as a result the shaft is lifted up which reduces the friction and eccentricity between shaft centre to bearing case centre. The main advantage of hydrostatic bearing are high load carrying capacity at any speed and no metal to metal contact at any range of speed so the chances of wear are almost neglected that increases the life of bearing (theoretically infinite).

In hydrostatic bearing it's load carrying capacity or stiffness does not depends on the viscosity of the lubrication so they are mostly used for non-viscous fluids including gases any cryogens.

LITERATURE REVIEW

Analysis is carried on how to reduce the drag force by controlling three different parameters of micro-cavity, i.e., depth, width and gap. Furthermore, they have analysed the various forces and pressure acting on the textured surfaces that are responsible for reduction of maximum drag force and finally the results are compared by numerically and experimentally [1]. Three-dimensional CFD simulations are used to investigate the pressure depression in aerostatic circular thrust bearing by numerically solving the Navier–Stokes equation for steady, 3D and compressible flows. The investigation shows that there exists a shock region when the flow occurs from supersonic flow to subsonic flow where relaminarization takes place [2]. The performance of aerostatic thrust bearing is presented under variable operating conditions with the help six orifice chambers having different shapes and configurations. By decreasing the air film thickness and increasing the spindle rotational speed in the analysis, the decrease in pressure depression, turbulent intensity and the load carrying capacity of the bearing is observed [3]. They have analysed the working of hydro-dynamically bearings that are lubricated by Bingham plastic fluids. The results were obtained in the form of Raimondi and Boyd graphs between normalized friction coefficient on bearing surface and Sommerfeld number. The results were obtained both for Newtonian fluid and Bingham fluid but Bingham fluid was more preferable because its load carrying capacity, frictional force are more compared to Newtonian fluid and increases with increases in dimensionless yield stress [4]. To detect the wear precisely in the bearing and journal mechanisms, CFD analysis is used to solve Navier–Stokes equation, and the diagrams for various bearing characteristics versus the Sommerfeld number is obtained for various wear depths. The graphical method presented is used for wear identification with the help of diagrams which are obtained in the results [5]. CFD method has been applied for the lubricant flow that to reduce the friction coefficient for the bearing having closed pockets. Analysis has been carried out for two types of bearing one with high convergence ratio and other with low convergence ratio. In high convergence ratio bearing a proper positioning of pocket in region where pressure is high that can results in reduction of shear stress which overall results in friction coefficient [6]. Results are obtained by both experimentally and by software analysis. Water lubricated journal bearing is to be designed considering properties of water and oil. Thickness of water film can be obtained from the derived equation and as per the film thickness bearing diameter can be selected. Eccentricity ratio plays an important role in designing the bearing which lies between 0.6 and 0.7 [7]. Analysis has been done in order to increase the load carrying capacity of bearing by introducing micro groove on

one of the two parallel surfaces. One of the walls is kept stationary and other moves with a specified tangential velocity and thus it increases the pressure and load carrying capacity of bearing. As the flow velocity of lubrication increases due to which its Reynolds number also increases that also results in increase the load carrying capacity of bearing but at certain velocity vortex appears and that point it gives maximum load carrying capacity of bearing [8]. As per this research paper, an extended Reynolds equation includes turbulence, convective inertia and temporal inertia. Due to the presence of convective inertia, it boosts the load capacity on bearing. In this experiment there is a use of low viscosity lubricant and high rotational speed. Lubricant with low viscosity is having good cooling capacity and low friction coefficient [9]. Using three-dimensional CFD techniques, a thermo hydrodynamics analysis on axially grooved fluid film journal bearing is presented. Energy equation of the lubricant flow, equations of heat conduction for the shaft and the bearing along with the full 3-D Navier–Stokes equation are used in order to carry out the analysis. By the method used in the paper, the temperature distribution along with pressure and velocity distributions in the cavitated region, for the flow of lubricant in the journal bearings are presented [10]. The viscosity of thin lubricant fluid is less as compared to thick lubricant. By using thin lubricant in journal bearing, the light weight load can only be lifted and hence thin lubricated journal bearing is not responsible for lifting heavy loads [11]. Three-dimensional CFD analysis is applied on a finite grooved journal bearing in a transient flow and the effects of journal misalignment are presented in the result. In the fluid dynamics simulations of an oil film, a different method is proposed in order to update the mesh volume during the movement of the journal bearings [12]. According to this paper, a method is given to calculate stiffness coefficient considering water as lubricant. As per the research the bearing size, diameter and etc is to be selected according to the working condition. Therefore water has a lubricant minimizes the cost compare to oil, good cooling performance, low friction coefficient due to the low viscosity of water [13]. Thermohydrodynamic performance of the bearing is analysed for different texture lengths. The texture has a stronger and positive influence on load carrying capacity when thermal effects are considered. Texture is related to load carrying capacity and load carrying capacity depends on sliding speed and inlet flow rate. The speed is depending upon roughness and smoothness. More the smoothness more will be the speed and more the roughness less will be the speed because of disturbance [14].

EQUATIONS

The Continuity Equation

Rate of accumulation of mass in the control volume + net rate of mass efflux from the control volume = 0 (1)

The rate of mass entering the control volume through face ABCD = ru dy dz and, the rate of mass leaving the control volume through face EFGH,

$$= \left(\rho + \frac{\partial \rho}{\partial x} dx\right)\left(u + \frac{\partial u}{\partial x} dx\right)\, dy\, dz$$

$= \left[\rho u + \frac{\partial}{\partial x}(\rho u) dx\right]\, dy\, dz$ (Neglecting higher order terms in dx)

Hence, the net rate of mass efflux from the control volume in the x direction.

$$= \left[\rho u + \frac{\partial}{\partial x}(\rho u) dx\right]\, dy\, dz - \rho u\, dy\, dz$$

$$= \frac{\partial}{\partial x}(\rho u)\, dx\, dy\, dz$$

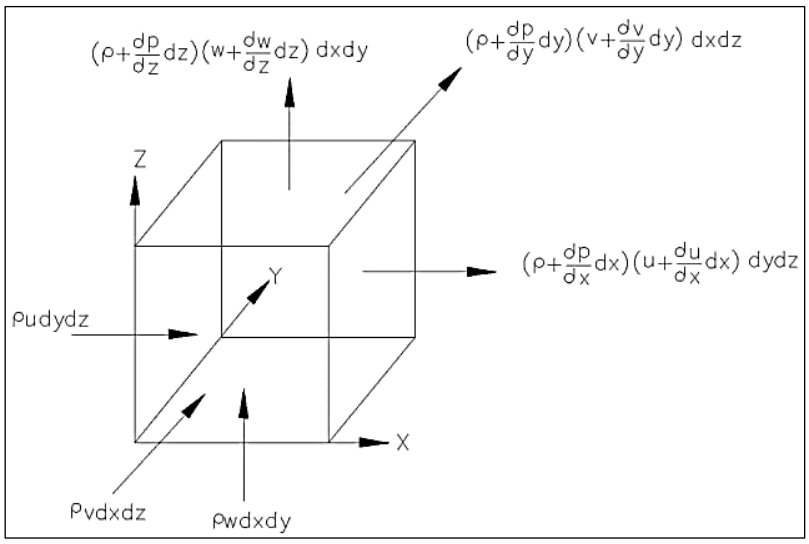

Fig. 2. *The continuity equation.*

$$= \frac{\partial}{\partial x}(\rho u)\, d\forall$$

Where, $d\forall$ is the elemental volume dx dy dz.

In a similar way, the net rate of mass efflux in the y direction. = $\frac{\partial}{\partial y}(\rho v)\, d\forall$

The net rate of mass efflux in the z direction = $\frac{\partial}{\partial z}(\rho w)\, d\forall$.

The rate of accumulation of mass within the control volume is $\frac{\partial}{\partial t}(\rho d\forall) = \frac{\partial \rho}{\partial t} d\forall$ (by definition of control volume, $d\forall$ is invariant with time). Therefore according to the statement of conservation of mass for a control volume (Eq.1), it can be written that

$$\left\{\frac{\partial \rho}{\partial t} + \frac{\partial}{\partial x}(\rho u) + \frac{\partial}{\partial y}(\rho v) + \frac{\partial}{\partial z}(\rho w)\right\} d\forall = 0$$

Since equation is valid irrespective of the size $d\forall$ of the control volume, we can write

$$\frac{\partial \rho}{\partial t} + \frac{\partial}{\partial x}(\rho u) + \frac{\partial}{\partial y}(\rho v) + \frac{\partial}{\partial z}(\rho w) = 0 \qquad (2)$$

This is well known equation of continuity of a compressible fluid in a rectangular Cartesian coordinate system. The equation can be written in a vector form as:

$$\frac{\partial \rho}{\partial t} + \nabla.\left(\rho \vec{V}\right) = 0 \qquad (3)$$

Where, $\vec{V}$ represents the velocity vector

In case of steady flow,

$$\frac{\partial \rho}{\partial t} = 0$$

Hence, Eq.(3) becomes

$$\nabla.\left(\rho \vec{V}\right) = 0 \qquad (4.a)$$

Or, in rectangular Cartesian coordinate system,

$$\frac{\partial}{\partial x}(\rho u) + \frac{\partial}{\partial y}(\rho v) + \frac{\partial}{\partial z}(\rho w) = 0 \qquad (4.b)$$

Equation Eq. (4.a), (4.b) represents the continuity equation for a steady flow. In case of an incompressible flow.

$$\rho = constant$$
$$hence\ {}^{\partial \rho}/_{\partial t} = 0\ and\ moreover\ \nabla.\left(\rho \vec{V}\right) = \rho \nabla.\left(\vec{V}\right)$$

Therefore, the continuity equation for an incompressible flow becomes

$$\nabla.\left(\vec{V}\right) = 0 \qquad (5)$$

$$\text{OR } \frac{\partial u}{\partial x} + \frac{\partial v}{\partial y} + \frac{\partial w}{\partial z} = 0 \qquad (6)$$

Navier–Stokes Equation

Consider a differential fluid element in the flow field. We wish to evaluate the surface forces acting on the boundary of this rectangular parallelepiped.

surface force on the surface BFGC per unit area is

$$\vec{F}_{sx} + \frac{\partial \vec{F}_{sx}}{\partial x}\, dx$$

Net force on the body due to imbalance of surface forces on the above two surfaces is,

$$\frac{\partial \vec{F}_{sx}}{\partial x}\, dx\, dy\, dz \qquad (7)$$

Total force on the body due to net surface forces on all six surfaces is,

$$\left(\frac{\partial \vec{F}_{sx}}{\partial x} + \frac{\partial \vec{F}_{sy}}{\partial y} + \frac{\partial \vec{F}_{sz}}{\partial z}\right) dx\, dy\, d \qquad (8)$$

and the resultant force dF per unit volume is,

$$d\vec{F} = \left(\frac{\partial \vec{F}_{sx}}{\partial x} + \frac{\partial \vec{F}_{sy}}{\partial y} + \frac{\partial \vec{F}_{sz}}{\partial z}\right) \qquad (9)$$

The quantities $\vec{F}_{SX}$, $\vec{F}_{SY}$ and $\vec{F}_{SZ}$ are vector which can be resolved into normal stresses and shearing stresses as:

$$\vec{F}_{sx} = \hat{\imath}\,\sigma_{xx} + \hat{\jmath}\,\tau_{xy} + \hat{k}\,\tau_{xz} \qquad (10a)$$

$$\vec{F}_{sy} = \hat{\imath}\,\tau_{yx} + \hat{\jmath}\,\sigma_{yy} + \hat{k}\,\tau_{yz} \qquad (10b)$$

$$\vec{F}_{sz} = \hat{\imath}\,\tau_{zx} + \hat{\jmath}\,\tau_{zy} + \hat{k}\,\sigma_{zz} \qquad (10c)$$

The stresses system is having nine scalar quantities. These nine quantities form a stress tensor. The set of nine components of stress tensor can be described as:

$$\pi = \begin{bmatrix} \sigma_{xx} & \tau_{xy} & \tau_{xz} \\ \tau_{yx} & \sigma_{yy} & \tau_{yz} \\ \tau_{zx} & \tau_{zy} & \sigma_{zz} \end{bmatrix} \qquad (11)$$

The above stress tensor is symmetric, which means that two shearing stresses with subscripts which differ only in their sequence are equal. Considering the equation of motion for instantaneous rotation of fluid element about y axis, we can write,

$$\dot{\omega}_y\, dI_y = (\tau_{xz}\, dy\, dz)\, dx - (\tau_{zx}\, dx\, dy)\, dz$$

$$\dot{\omega}_y\, dI_y = (\tau_{xz} - \tau_{zx})\, d\forall$$

Where, d∀ is the volume of the element, and $\dot{\omega}_y$ and dI_y are the angular acceleration and moment of inertia of the element about y-axis respectively. Since dI_y is proportional to the fifth power of the linear dimension and dV is proportional to the third power of the linear dimension, the left hand side of the above equation vanishes faster than the right hand side on contracting the element to a point. Hence the result is,

$$\tau_{xz} = \tau_{zx}$$

From the similar consideration about other two remaining axis, we can write,

$$\tau_{xy} = \tau_{yx}$$

$$\tau_{yz} = \tau_{zy}$$

Invoking the above condition now the stress tensor becomes:

$$\pi = \begin{bmatrix} \sigma_{xx} & \tau_{xy} & \tau_{xz} \\ \tau_{xy} & \sigma_{yy} & \tau_{yz} \\ \tau_{xz} & \tau_{yz} & \sigma_{zz} \end{bmatrix} \qquad (12)$$

Combining the equation (9), (10a), (10b), and (10c), the resultant force per unit volume becomes:

$$d\vec{F} = \hat{\imath}\left(\frac{\partial \sigma_{xx}}{\partial x} + \frac{\partial \tau_{xy}}{\partial y} + \frac{\partial \tau_{xz}}{\partial z}\right) + \hat{\jmath}\left(\frac{\partial \tau_{xy}}{\partial x} + \frac{\partial \sigma_{yy}}{\partial y} + \frac{\partial \tau_{yz}}{\partial z}\right) + \hat{k}\left(\frac{\partial \tau_{xz}}{\partial x} + \frac{\partial \tau_{yz}}{\partial y} + \frac{\partial \sigma_{zz}}{\partial z}\right) \qquad (13)$$

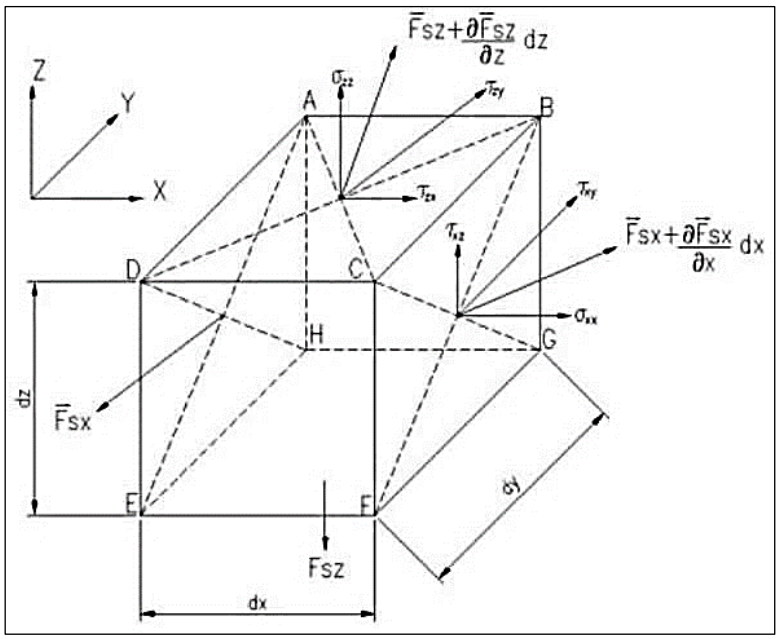

Fig 3. *Navier–Stokes Equation*

As per the velocity field

$$\frac{D\vec{V}}{Dt} = \hat{\imath}\frac{D_u}{Dt} + \hat{\jmath}\frac{D_v}{Dt} + \hat{k}\frac{D_w}{Dt} \qquad (14)$$

By Newton's Law of motion applied to the differential element, we can write

$$\rho(dx\,dy\,dz)\frac{D\vec{V}}{Dt} = \left(d\vec{F}\right)(dx\,dy\,dz) + \rho\vec{f_b}(dx\,dy\,dz)$$

$$OR\ \rho\frac{D\vec{V}}{Dt} = d\vec{F} + \rho\vec{f_b}$$

Substituting equation (13),(14) in the above expression and expressing $\frac{Du}{Dt}, \frac{Dv}{Dt}, \frac{Dw}{Dt}$ in terms of field derivatives further we obtain,

$$\rho\frac{Du}{Dt} = \rho f_x - \frac{\partial p}{\partial x} + \frac{\partial}{\partial x}\left[\mu\left(2\frac{\partial u}{\partial x} - \frac{2}{3}\nabla.\vec{V}\right)\right] + \frac{\partial}{\partial y}\left[\mu\left(\frac{\partial u}{\partial y} + \frac{\partial v}{\partial x}\right)\right] + \frac{\partial}{\partial z}\left[\mu\left(\frac{\partial w}{\partial x} + \frac{\partial u}{\partial z}\right)\right] \qquad (15a)$$

$$\rho\frac{Dv}{Dt} = \rho f_y - \frac{\partial p}{\partial y} + \frac{\partial}{\partial y}\left[\mu\left(2\frac{\partial v}{\partial y} - \frac{2}{3}\nabla.\vec{V}\right)\right] + \frac{\partial}{\partial z}\left[\mu\left(\frac{\partial v}{\partial z} + \frac{\partial w}{\partial y}\right)\right] + \frac{\partial}{\partial x}\left[\mu\left(\frac{\partial u}{\partial y} + \frac{\partial v}{\partial x}\right)\right] \qquad (15b)$$

$$\rho\frac{Dw}{Dt} = \rho f_z - \frac{\partial p}{\partial z} + \frac{\partial}{\partial z}\left[\mu\left(2\frac{\partial w}{\partial z} - \frac{2}{3}\nabla.\vec{V}\right)\right] + \frac{\partial}{\partial x}\left[\mu\left(\frac{\partial w}{\partial x} + \frac{\partial u}{\partial z}\right)\right] + \frac{\partial}{\partial y}\left[\mu\left(\frac{\partial v}{\partial z} + \frac{\partial w}{\partial y}\right)\right] \qquad (15c)$$

Now equation of continuity for the incompressible flow is

$$\frac{\partial u}{\partial x} + \frac{\partial v}{\partial y} + \frac{\partial w}{\partial z} = 0 \qquad (16)$$

Invoking equation (16) into equation (15a), (15b), and (15c) we get

$$\rho\left(\frac{\partial u}{\partial t} + u\frac{\partial u}{\partial x} + v\frac{\partial u}{\partial y} + w\frac{\partial u}{\partial z}\right) = \rho f_x - \frac{\partial p}{\partial x} + \mu\left(\frac{\partial^2 u}{\partial x^2} + \frac{\partial^2 u}{\partial y^2} + \frac{\partial^2 u}{\partial z^2}\right) \qquad (17a)$$

$$\rho\left(\frac{\partial v}{\partial t} + u\frac{\partial v}{\partial x} + v\frac{\partial v}{\partial y} + w\frac{\partial v}{\partial z}\right) = \rho f_y - \frac{\partial p}{\partial y} + \mu\left(\frac{\partial^2 v}{\partial x^2} + \frac{\partial^2 v}{\partial y^2} + \frac{\partial^2 v}{\partial z^2}\right) \qquad (17b)$$

$$\rho\left(\frac{\partial w}{\partial t} + u\frac{\partial w}{\partial x} + v\frac{\partial w}{\partial y} + w\frac{\partial w}{\partial z}\right) = \rho f_z - \frac{\partial p}{\partial z} + \mu\left(\frac{\partial^2 w}{\partial x^2} + \frac{\partial^2 w}{\partial y^2} + \frac{\partial^2 w}{\partial z^2}\right) \qquad (17c)$$

In short, vector notation may be used to write Navier-Stoke and continuity equation for incompressible flow as:

$$\rho \frac{D\vec{V}}{Dt} = \rho \vec{f_b} - \nabla p + \mu \nabla^2 \vec{V} \quad (18)$$

METHODOLOGY

In order to get the results, we must have the governing differential equations which in this case are momentum and continuity equations,

$$\rho \frac{\Delta \vec{V}}{\Delta t} = -\nabla p + \mu \nabla^2 \vec{u} + \rho \vec{F} \quad (19)$$

Assuming τ α ϕ, inertia term and body force term are very less as compared to viscous term with laminar flow as Reynolds number is very less for such kind of flows.

$$\frac{\Delta \rho}{\Delta t} = 0 \quad (20)$$

Utilizing the assumptions, equation (1) and (2) gets reduced to the following forms:

$$\left(u\frac{\partial u}{\partial x} + v\frac{\partial v}{\partial y} + w\frac{\partial w}{\partial z}\right)\rho = -\frac{\partial p}{\partial x} + \mu\left(\frac{\partial^2 u}{\partial x^2} + \frac{\partial^2 u}{\partial y^2} + \frac{\partial^2 u}{\partial z^2}\right) \quad (21)$$

$$\frac{\partial u}{\partial x} + \frac{\partial v}{\partial y} + \frac{\partial w}{\partial z} = \quad (22)$$

In order to find out one-dimensional analytical solution, order of magnitude method is to be applied. Let V, L be velocity and length (maximum possible),

Therefore, u, v~ V, x, y ~ l.
Z-direction (height direction) ~ H,
Pressure p ~ P and equation (3) can be converted to,

$$\frac{\rho V^2}{l} = -\frac{P}{l} + \frac{\mu V}{l^2} + \frac{\mu V}{H^2} \quad (23)$$

Dividing equation (5) by $\frac{\mu V}{H^2}$

$$-\frac{\partial P}{\partial x} + \mu \frac{\partial^2 u}{\partial z^2} = 0 \text{ (x-component)} \quad (24)$$

$$-\frac{\partial P}{\partial y} + \mu \frac{\partial^2 v}{\partial z^2} = 0 \text{ (y-component)} \quad (25)$$

$$-\frac{\partial P}{\partial x} = 0 \qquad p \neq f(z) \quad (26)$$

$$u = C_1 + C_2 z + \frac{z^2}{2\mu}\frac{\partial P}{\partial x} \quad (27)$$

We need 2 boundary conditions,
At z=0, u=0,
At z=H, u=0.

$$\therefore u = \frac{1}{2\mu}\frac{\partial P}{\partial x}(z^2 - 2H) \quad (28)$$

Similarly for y component,

$$v = \frac{1}{2\mu}\frac{\partial P}{\partial y}(z^2 - 2H) \quad (29)$$

Since we got the velocity profiles, but no pressure distribution (which is our matter of concern), we have continuity equation for 2D.

Using Leibnitz rule and above equations become,

$$\int_0^H \left(\frac{\partial u}{\partial x} + \frac{\partial v}{\partial y}\right) dz = 0$$

$$\frac{1}{2\mu}\left[\frac{\partial^2 P}{\partial y^2} + \frac{\partial^2 P}{\partial x^2}\right]\int_0^H (z^2 - 2H)dz = 0$$

$$\frac{\partial^2 P}{\partial x^2} + \frac{\partial^2 P}{\partial y^2} = 0 \quad (30)$$

For ID, we have,
Q = Area × Velocity (discharge)

$$Q = \int_0^H (ub)dz \quad (31)$$

Substituting value of velocity,

$$Q = \frac{(P_1 - P_2)bH^3}{12\mu l} \quad (32)$$

dp → Δp and dx→L on integration in Cartesian coordinates.
b→2πr and Δp → dp (cylindrical coordinates)

$$P = \ln r(\pi H^3)^{-1}(-\mathbf{6}\mu Q) + C$$

P (r_0) = P_i

$$Q = P_i\pi(H^3)\left[\ln\left(\frac{r}{r_0}\right)6\mu\right]^{-1} \quad (33)$$

Total load,

$$W = P_i(\pi {r_0}^2) + \int_{r_0}^{r} P(2\pi r)dr$$

$$\therefore W = \frac{P_i\pi}{2}(r^2 - {r_0}^2) + \left[\ln\frac{r}{r_0}\right]^{-1} \quad (34)$$

Work required for the pump to force in lubricant or oil in the recess depends on the pressure difference given as follows:
$Q \times (P_1 - P_2)$

The additional work to be done by the pump is the work done due to friction power is given by (due to friction).

$$P_{friction} = \left(\frac{2\pi NT}{60}\right) \rightarrow \left(\frac{2\pi N}{60} \times force \times radius\right)$$

$$= \frac{2\pi N}{60} \times \int_{r_0}^{r} \frac{\mu rw}{h} 2\pi r dr \times \frac{\mu \times rw}{h} \quad (35)$$

$$= \frac{2\mu}{h} \times \frac{\pi^3}{4} \times \left(\frac{2N}{60}\right)^2 \times (r^2 - {r_0}^2) \quad (36)$$

This completes the analytical part, for ID pressure distribution

$$\frac{\partial^2 P}{\partial x^2} = 0$$

$$\frac{P_{i+1} + P_{i-1} - 2P_i}{(\Delta x)^2} = 0 \text{ (Central difference scheme)} \quad (37)$$

$$u = \frac{1}{2\mu}\frac{dP}{dx}(z^2 - 2H) \quad (38)$$

$$\therefore \int_0^W \int_0^H \left[\frac{1}{2\mu}\frac{dP}{dx}(z^2 - 2H)\right] dzdy$$

$$= \frac{WH^3}{12\mu}\left(-\frac{\partial P}{\partial x}\right) \quad (39)$$

$$v = \frac{1}{2\mu}\frac{dP}{dy}(z^2 - 2H) \quad (40)$$

$$\therefore \int_0^L \int_0^H \left[\frac{1}{2\mu}\frac{dP}{dy}(z^2 - 2H)\right] dzdx \quad (41)$$

y- direction flow rate,

$$= \left(\frac{dP}{dy}\right)(L)\left(-\frac{h^3}{12\mu}\right) \quad (42)$$

Load calculation,

$$W_{recess} + W = P_i l_{recess} W_r + \int_{Area} P dxdy \quad (43)$$

$$\left(\frac{\partial^2 P}{\partial x^2}\right) + \left(\frac{\partial^2 P}{\partial y^2}\right) = 0 \quad \text{….. (g)}$$

$$\frac{P_{i+1,j} + P_{i-1,j} - 2P_{i,j}}{(\Delta x)^2} + \frac{P_{j+1,i} + P_{j-1,i} - 2P_{i,j}}{(\Delta y)^2} = 0 \quad (44)$$

$P = \frac{\mu UL}{H^2}$ (by order of magnitude method)

$$\therefore -\frac{\partial P}{\partial x} + \mu\frac{\partial^2 u}{\partial z^2} = 0$$

RESULTS AND CONCLUSION:

All results has been shown in tabulated form. For a given pressure, the power required is more as the height increases. This is observed from results obtained from Table 1-2 as listed below.

(a) For pressure P = 4998.70 kPa
Load = 582.18 kN
Flow rate coefficient = 0.519
(b) For pressure P = 5171.07 kPa
Load = 602.245 kN
Flow rate coefficient = 0.519

Table 1. *For a given pressure 4998.70 kPa, the power required is more as the height increases.*

Height (m)	Q (m^3/s)	Load coefficient	Power (W)	Temperature difference
2.54E-05	1.64E-05	180.52	0.670	-14.97
7.62E-05	3.82E-06	180.52	19.09	-14.97
1.27E-04	1.77E-05	180.52	88.55	-14.97
1.78E-04	4.86E-05	180.52	242.97	-14.97
2.29E-04	1.03E-04	180.52	516.45	-14.97

Table 2. *For a given pressure 5171.07 kPa, the power required is more as the height*

Height (m)	Q (m^3/s)	Load coefficient	Power (W)	Temperature difference
2.54E-05	1.64E-05	180.52	0.746	-14.87
7.62E-05	3.97E-06	180.52	20.44	-14.87
1.27E-04	1.83E-05	180.52	94.74	-14.87
1.78E-04	5.03E-05	180.52	260.05	-14.87
2.29E-04	1.07E-04	180.52	552.71	-14.87

Further, by increasing the load along with pressure, pump power increases. Similarly, by varying the pressure and load, the change is other parameters are noted in the following result table 3-5.

Table 3. *For a given pressure 5343.437 kPa the power required is more as the height*

Height (m)	Q (m^3/s)	Load coefficient	Power (W)	Temperature difference
2.54E-05	1.64E-05	180.52	0.8206	-14.77
7.62E-05	4.10E-06	180.52	21.85	-14.77
1.27E-04	1.89E-05	180.52	101.15	-14.77
1.78E-04	5.19E-05	180.52	277.66	-14.77
2.29E-04	1.10E-04	180.52	590.16	-14.77

(c) For pressure P = 5343.437 kPa
Load = 622.306 kN
Flow rate coefficient = 0.519

(d) For pressure P = 5515.806 kPa
Load = 642.412 kN
Flow rate coefficient = 0.519

(e) For pressure P = 5860.544 kPa
Load = 662.473 kN
Flow rate coefficient = 0.519

Table 4. *For a given pressure P = 5515.806 kPa the power required is more as the height*

Height (m)	Q (m^3/s)	Load coefficient	Horse power	Temperature difference
2.54E-05	1.64E-07	180.52	0.8952	-14.68
7.62E-05	4.23E-06	180.52	23.2752	-14.68
1.27E-04	1.95E-05	180.52	107.797	-14.68
1.78E-04	5.36E-05	180.52	295.863	-14.68
2.29E-04	1.14E-04	180.52	628.878	-14.68

Table 5. *For a given pressure P = 5860.544 kPa the power required is more as the height*

Height (m)	Q (m^3/s)	Load coefficient	Power (W)	Temperature difference
2.54E-05	1.64E-07	180.52	0.8952	-14.58
7.62E-05	4.36E-06	180.52	24.76	-14.58
1.27E-04	2.02E-05	180.52	114.66	-14.58
1.78E-04	5.53E-05	180.52	314.66	-14.58
2.29E-04	1.18E-04	180.52	668.78	-14.58

CONCLUSION

1. As per the results, it is observed that with increase in pressure and corresponding load, the volumetric flow rate increases.
2. With increase in volumetric flow rate, the corresponding pump power also increases.
3. With increase in pressure and load, the temperature difference between the oil and surrounding increases.

REFERENCES

[1] Caramia G, Carbone G, De Palma P. Hydrodynamic lubrication of micro-textured surfaces: Two dimensional CFD-analyses. *Tribology International.* 2015; *88:* 162–169p.

[2] Eleshaky ME. CFD investigation of pressure depressions in aerostatic circular thrust bearings. *Tribology International.* 2009; 42(7): 1108–1117p.

[3] Gao S, Cheng K, Chen S, Ding H, Fu H. CFD based investigation on influence of orifice chamber shapes for the design of aerostatic thrust bearings at ultra-high speed spindles. *Tribology international.* 2015; 92: 211–221p.

[4] Gertzos KP, Nikolakopoulos PG, Papadopoulos CA.. CFD analysis of journal bearing hydrodynamic lubrication by Bingham lubricant. *Tribology International.* 2008; 41(12): 1190–1204p.

[5] Gertzos KP, Nikolakopoulos PG, Chasalevris AC, Papadopoulos CA. Wear identification in rotor-bearing systems by measurements of dynamic bearing characteristics. *Computers & Structures.* 2011; 89(1–2): 55–66p.

[6] Brajdic-Mitidieri P, Gosman AD, Ioannides E, Spikes HA. CFD analysis of a low friction pocketed pad bearing. *Journal of Tribology.* 2005; 127(4): 803–812p.

[7] Gao G, Yin Z, Jiang D, Zhang X. Numerical analysis of plain journal bearing under hydrodynamic lubrication by water. *Tribology International.* 2014; 75: 31–38p.

[8] Sahlin F, Glavatskih SB, Almqvist T, Larsson R. Two-dimensional CFD-analysis of micro-patterned surfaces in hydrodynamic lubrication. *Journal of Tribology.* 2005; 127(1): 96–102p.

[9] Dousti S, Allaire P, Dimond T, Cao J.. An extended Reynold equation applicable to high reduced Reynolds number operation of journal bearings. *Tribology International.* 2016; 102: 182–197p.

[10] Nassab SG, Moayeri MS. Three-dimensional thermohydrodynamic analysis of axially grooved journal bearings. *Proceedings of the Institution of Mechanical Engineers, Part J: Journal of Engineering Tribology.* 2002; 216(1): 35–47p.

[11] Manshoor B, Jaat M, Izzuddin Z, Amir K. CFD analysis of thin film lubricated journal bearing. *Procedia Engineering.* 2013; *68:* 56–62p.

[12] Li Q, Liu SL, Pan XH, Zheng SY. A new method for studying the 3D transient flow of misaligned journal bearings in flexible rotor-bearing systems. *Journal of Zhejiang University Science A.* 2012; 13(4), 293–310p.

[13] Zhang X, Yin Z, Gao G, Li Z.. Determination of stiffness coefficients of hydrodynamic water-lubricated plain journal bearings. *Tribology International.* 2015; 85: 37–47p.

[14] Cupillard S, Glavatskih S, Cervantes MJ. 3D thermohydrodynamic analysis of a textured slider. *Tribology international.* 2009; 42(10): 1487–1495p.